Anal. Bioanal. Electrochem., Vol. 11, No. 5, 2019, 657-667

Analytical & Bioanalytical Electrochemistry

2019 by CEE
www.abechem.com

Full Paper

Superparamagnetic Nanoparticles Doped with Copper Cations and Surface-Capped by Polyvinylpyrrolidone for Biomedical Applications

Isa Karrimzadeh[1,*] and Mohammad Faryadi [2]

[1]*Department of Physics, Faculty of Science, Central Tehran Branch, Islamic Azad University, Tehran, Iran*

[2]*Materials and Nuclear Research School, Nuclear Science and Technology Research Institute (NSTRI), P.O. Box 14395-834, Tehran, Iran*

*Corresponding Author, Tel.: +98-21-44356639; Fax: +98-21-44356639

E-Mail: isa.karimzadeh@gmail.com

Received: 11 January 2019 / Received in revised form: 25 March 2019 / Accepted: 5 April 2019 / Published online: 31 May 2019

Abstract- In this paper, we report well-dispersed superparamagnetic magnetite nanoparticles (SPMNs) surface-capped with polyvinylpyrrolidone (PVP) and structure-doped by Cu(II) ions. The SMNPs powder was obtained though galvanostatic two-electrode cathodic electrochemical synthesis. The prepared SPMNs samples were characterized via the structural and magnetical techniques of FE-SEM, EDS, TEM, XRD, FT-IR, and VSM. The magnetic data measured though VSM technique revealed superparamagnetic nature for the PVP-capped Cu-IONs sample, where relative high saturation magnetization, low remanence and negligible coercivity (i.e. *Ms*=45.01 emu/g, *Mr*=0.49 emu/g and *Ce*=7.3 Oe) were obtained for this sample. In the FT-IR data, all adsorption bands related the PVP polymer i.e. carbon-hydrogen, carbon-oxygen and carbon-nitrogen were detected and proved the surface-capped feature of the deposited iron oxide particles. It was also found that the fabricated magnetic powder had pure magnetite crystal structure doped by about 7.5%wt. copper cations and fine particle size of 5nm. Based on these results, the designed electrochemical procedure was introduced as an efficient and low cost synthetic way for fabricating the surface-capped metal cations doped magnetite ultra-fine particles.

Keywords - Surface coating, Metal-ion doping, Magnetite particles, Electrochemical synthesis

1. INTRODUCTION

Recently, iron oxides (IOs) had been proper candidates for use in biomedical aims as the results of their suitable magnetic characters (i.e. high saturation magnetization, low remanence and negligible coercivity), simple and low coat fabrication, easy surface functionalization, colloidal stability, ideal biocompatibility (i.e. low natural toxicity and cell toxicity) and magnetothermal effect [1-9]. The most common biomedical uses of IOs include magnetic resonance imaging (MRI) [10,11], hyperthermia [12,13], drug delivery [14,15] and bio-sensing [16]. These oxides are currently investigated for environmental applications like removal of heavy metals contamination from the water [17-19], and catalysis role in organic synthesis [20,21] due to their high active surfaces, high surface area and mixed valance states. Furthermore, IOs are extensively studied for application as electro-active material in charge storage devices like batteries and supercapacitors [22-27]. Nanoparticles of magnetite (Fe_3O_4), hematite (α-Fe_2O_3) and maghemite (γ-Fe_2O_3) are the three most common nanostructures of iron oxides. Among these structures, nanoparticles of superparamagnetic iron oxides (SPIOs) have earned most interest for the above listed uses as the advantages of their natural abundance, lower toxicity, mixed oxidation states, lower cost, the environmental friendliness, better superparamagnetim and easy surface engineering as compared with other iron oxides i.e. hematite and maghemite [28,29]. Hence, many research groups including materialist, chemists, biochemists, bioengineers and medical physicians have tied to fabricate nanoparticles of SPIOs with requested criteria and characteristics, and study their biomedical performance. And, some efficient and easy chemical procedures like solvothermal [30], thermal decomposition [31,32], hydrothermal [33] and co-precipitation [34,35], have been established for prepare IOs nanoparticles, with suitable crystalline nature (i.e. pure magnetite phase), spherical shape (i.e. particle morphology), narrow distribution (i.e. uniform particles), controlled particle size (i.e. below 100nm), and requested magnetic ability (i.e. negligible *Mr*, high *Ms* and low *Ce*). Furthermore, different surface coating techniques including chemisorption, direct nanoparticle conjugation, covalent linker chemistry, ligand exchange and physical interactions) have been developed to prepared surface-capped IOs with enhanced biocompatibility, stability, and solubility, and decreased surface charge [36-38]. However, most of these strategies have been reported suffer from limitations like as low stability, complex, poor biocompatibility, difficult and multistep synthesis steps and hydrophobic products. Among these routes, coating procedures based on ligand exchange and chemisorption has been reported to be a suitable way to easy surface functionalization of IOs with biocompatible agents [38]. For surface-capping of iron oxide nanoparticles (IONs), a variety of biocompatible biomolecules, natural and synthetic polymers have been used which include amino acids [39,40], polyvinylpyrrolidone [41-43], dextran [44,45], polyethylenimine [46], chitosan [47], polyvinyl alcohol [48,49] and saccharides [50,51].

Cathodic electrodeposition, as an electrochemical deposition mode, provides a simple fabrication method for the obtaining nano-scale oxides/hydroxides with sheet- [52,53], rod- [54-56], particle- [57-59], plate-like [60,61] morphologies and also oxide/hydroxide@carbon nanocomposites [62-64]. These advantages referred to the simple controlling parameters like current, voltage, concentration, temperature and pH applicable in the deposition experiments. Furthermore, the electrochemical fabrication uses the mild conditions and low cost devices and precursors to achieve final products [65]. In cathodic electrodeposition method, the final deposits (i.e. products) are electrochemically formed *via* an EC mechanism. In this way, hydroxyl anions are firstly electro-generated in the cathode side and then reacted with metal cations [65]. About electrochemical synthesis of IONs, cathodic electrodeposition has been used as simple way for synthesis of naked IONs in both aqueous and organic deposition baths and their *in-situ* surface-capping with biocompatible agents [66-71]. In this paper, superparamagnetic polyvinylpyrrolidone-capped copper-doped IONs (i.e. PVP/Cu-IONs powder) are prepared through one-step, low-cost and efficient cathodic electrodeposition for the first time. The fabricated PVP/Cu-IONs was studied *through* TEM, XRD, FT-IR, FE-SEM, EDS and VSM techniques, and the obtained data were discussed in detail.

2. EXPERIMENTAL PART

2.1. Chemicals

$Cu(NO_3)_2$ $3H_2O$ (Merck Millipore, M_w=240.2 g/mol), $FeCl_3$ $6H_2O$ (Merck Millipore, M_w=270.3 g/mol), $FeCl_2$ $4H_2O$ (Merck Millipore, M_w=198.8 g/mol, 99.9%), and polyvinylpyrrolidone (PVP, Merck Millipore) were purchased and used as received.

2.2. Preparation of samples

The magnetic samples were obtained using the well-known cathodic electrochemical deposition procedure reported in Refs. [72,73]. A two-electrode cell linked to the DC power supply (PROVA-8000) was constructed as the deposition set up. The volume of the electrochemical cell was one litter. The electrodes were selected to be two 304 stainless steel with dimensions of 5 cm width and 10 cm length. One litter electrolyte of 3 g iron(III) chloride, 1.5 g iron(II) chloride, 0.5 g copper(II) chloride and 0.5 g polymer (i.e. PVP) dissolved in ethanol was prepared and used. Using DC power supply, the current density of 0.1 A/cm^2 was applied into the deposition cell for 10min and the black deposit was observed onto the cathode electrode. Then, the electrode was removed from the electrolyte and washed with ethanol for 10 times. The observed film was separated from the surface of steel electrode and the obtained wet powder was dried in 80 ^oC RT for 5h to evaporate the ethanol electrolyte. The prepared dry powder was labeled PVP/Cu-IONs product.

2.3. Characterization techniques

The morphological images of the prepared samples were provided by instrument of field-emission scanning and transmission electron microscopies i.e. Mira 3-XMU FE-SEM and Zeiss EM900 TEM. Furthermore, the elemental composition of PVP/Cu-IONs sample was examined through energy dispersive diffraction X-ray analyzer assembled onto the FE-SEM microscope, and EDS data was obtained. The crystallographic XRD patterns of the samples were taken by Phillips PW-1800 XRD instrument and also crystallite size (D) of the samples was calculated via Scherer equation using (311) diffraction. Chemical composition of the samples was investigated by FTIR analysis to prove the polymer layer onto Cu-IONs particles, and the IR spectrum was recorded using a Bruker Vector 22 FT-IR instrument at the range of 400 -4000 cm^{-1}. VSM assessments were performed on Lakeshore 7400 series instrument, and the hysteresis profile was measured at −20000Oe to +20000 Oe, and then magnetic values of saturation magnetization (*Ms*), remanence (*Mr*) and coercivity (*Ce*) were obtained using the VSM graphs.

3. RESULTS AND DISCUSSION

3.1. Crystal structure of the samples

Fig. 1 presents X-ray powder diffraction pattern of the obtained PVP/Cu-IONs. As shown in Fig. 1, entire diffractions observed in this XRD pattern are fully matched with the Fe_3O_4 diffractions with cubic crystal structure (reference number 01-088-0315). No additional diffractions elated to the other oxide phases (i.e. hematite or maghemite) were observed, which proofed the purity for the fabricated PVP/Cu-IONs sample. As, no change in the crystal structure of iron oxide is detected hence it is confirmed that the copper cations have substituted in the octahedral site related to the Fe^{2+} cations in the crystal structure of the magnetite phase of iron oxide. Also, the average crystallite size (D) of 5.2 nm was calculated for our prepared particles *via* the Scherrer's equation ($D=0.9\lambda/\beta \cos(\theta)$) and data related to the main diffraction peak of PVP/Cu-IONs (i.e. (311) peak).

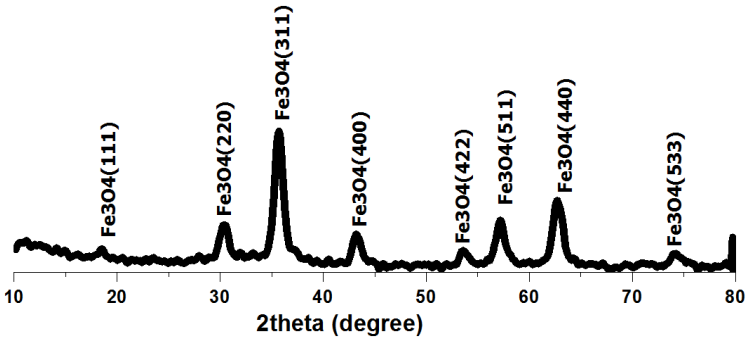

Fig. 1. XRD pattern of the Cu-IONs sample

3.2. Morphology and particle size

Morphological images (provided *via* FE-SEM and TEM instruments) and also elemental composition data of the prepared PVP/Cu-IONs are shown in Fig. 2. The FE-SEM image in Fig. 2a presents spherical colonies composed of fine copper doped iron oxide particles. The observed particles exhibited complete uniform sphere with size less than 10 nm. TEM observation provided in Fig. 2b indicated uniform ultrafine particles with sizes of about 5nm in size (Fig. 2b).

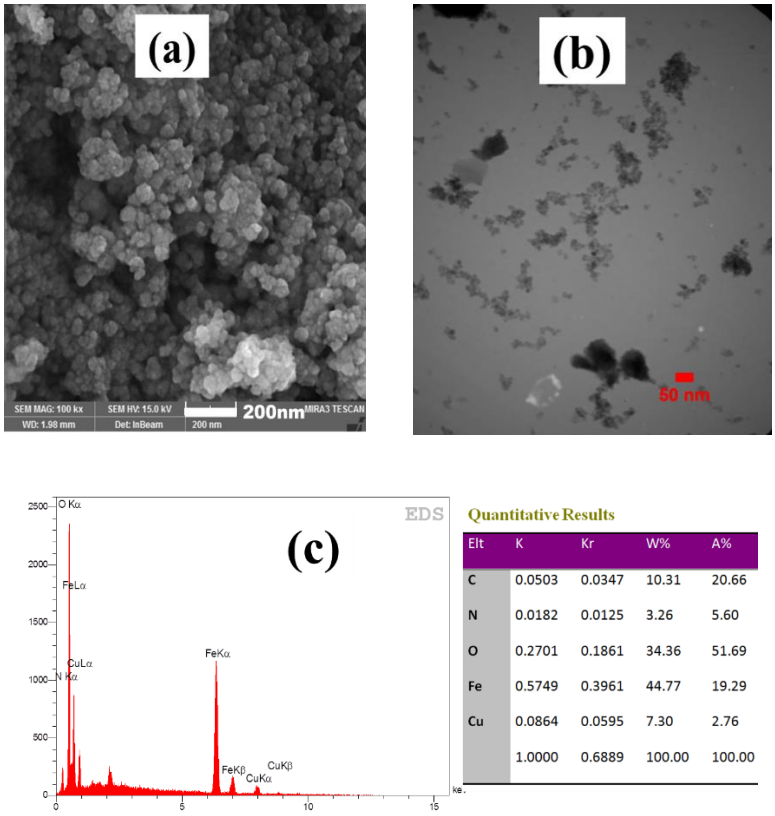

Elt	K	Kr	W%	A%
C	0.0503	0.0347	10.31	20.66
N	0.0182	0.0125	3.26	5.60
O	0.2701	0.1861	34.36	51.69
Fe	0.5749	0.3961	44.77	19.29
Cu	0.0864	0.0595	7.30	2.76
	1.0000	0.6889	100.00	100.00

Fig. 2. (a) FE-SEM; (b) TEM images and (c) EDS data of the obtained Cu^{2+}-doped PVP-grafted IONs

The elemental composition of the PVP/Cu-IONs powder was evaluated by EDS analysis and the obtained profile is given in Fig. 2c. It can be seen that the presence of the presence of C, N, O, Cu and Fe confirmed to be exists in the composition of prepared powder (Fig. 2c). The weight percentage (wt.%) and atomic percentage (A%) related to these elements i.e. C, O, Fe, Cu and N are also presented in Fig. 2d. It was obtained that the carbon elements include the 10.31%wt. and 20.66 %A of the fabricated powder. Furthermore, the N elements make up the 3.26%wt. and 5.6%A of sample composition. The presence of these two elements indicated the PVP layer onto the surface of the synthesized iron oxide nanoparticles. For the copper cations, the values of weight percentage (wt.%) and atomic percentage (A%) were measured

to be 7.3%wt. and 2.76%A, respectively, indication the doping of the deposited iron oxide by 7.3% Cu^{2+} cations. Furthermore, the iron element with weight percentage of 44.77% wt. and oxygen with 34.36% wt. revealed the Fe3O4 nature for the prepared powder. In final, the fine particle surface feature, 5 nm particle size, PVP capped and 7.3%wt. doped with Cu^{2+} cations were confirmed *via* the results of FE-SEM, TEM and EDS analyses.

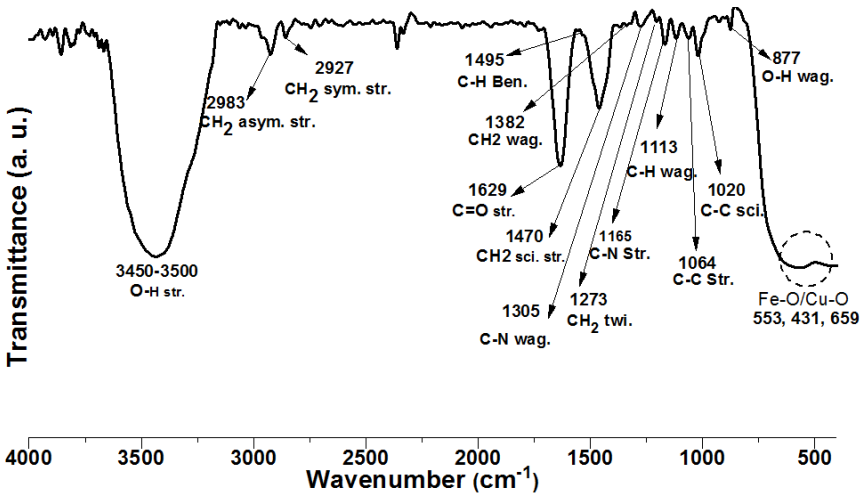

Fig. 3. IR spectrum of the obtained Cu^{2+} doped PVP-grafted IONs

3.3. FT-IR

The chemical composition of the synthesized PVP/Cu-IONs powder was evaluated through FT-IR instrument and the IR spectrum of the prepared PVP/Cu-IONs particles was obtained in the wavenumbers of 400-4000 cm^{-1} as given in Fig. 3. The IR bands at the wavenumbers below 700 cm^{-1} are assigned to the stretching mods of M-O-M chemical bonds [69,70]. In this zone, two IR bands observed at 553 cm^{-1} and 659 cm^{-1} are due to splitting of the ν_1 mode vibrations of the Fe^{2+}—O^{2-}/Cu^{2+}—O^{2-} chemical bonds [64-66], a IR band at 431 cm^{-1} is due to the ν_2 vibration mode of the Fe^{3+}—O^{2-} chemical bonds [64,65]. At higher wavenumbers, different IR peaks are observed, which can be assigned to the following chemical bonds vibrations [42-44]: $\nu_{stretching}$ of –OH groups at 3450-3500 cm^{-1}, $\nu_{asymmetric\ stretching}$ of CH_2 groups 2983 cm^{-1} for, $\nu_{symmetric\ stretching}$ of CH_2 groups at 2927 cm^{-1}, $\nu_{stretching}$ of C=O groups at 1629 cm^{-1}, $\nu_{scissoring}$ of CH_2 groups at 1473 cm^{-1}, $\nu_{bending}$ of C-H bonds at 1495 cm^{-1} for, $\nu_{wagging}$ of CH_2 groups at 1382 cm^{-1}, $\nu_{wagging}$ of C-N bonds at 1305 cm^{-1}, $\nu_{twisting}$ of CH_2 groups at 1273 cm^{-1}, , $\nu_{stretching}$ of C-N bonds at 1165 cm^{-1}, $\nu_{wagging}$ of C-H bonds at 1163 cm^{-1}, $\nu_{wagging}$ of C-H bonds at 1113 cm^{-1}, $\nu_{stretching}$ of C-C bonds at 1064 cm^{-1}, $\nu_{scissoring}$ of C-C bonds at 1020 cm^{-1}, and $\nu_{wagging}$ of O-H bonds at 877 cm^{-1}. Notably, it was reported that the $\nu_{stretching}$ of C=O groups is seen at 1660 cm^{-1} for pure PVP [42]. In the case of PVP/Cu-Ions, C=O chemical bond vibration has been shift from 1660 cm^{-1} to 1629 cm^{-1}. This indicated the chemical connection of C=O groups of PVP

with iron oxide, and proved the surface grafting Cu-IONs with PVP layer. Hence, the IR spectrum exhibited $\nu_{stretching}$, $\nu_{scissoring}$ and $\nu_{wagging}$ of all chemical bands and related groups related to the PVP and Cu-doped Fe_3O_4, which include C-C, C=O, C-N, C-H, Fe-O, Cu-O, –OH and -CH_2 groups. These IR data verified the expected chemical composition for the synthesized PVP/Cu-IONs powder.

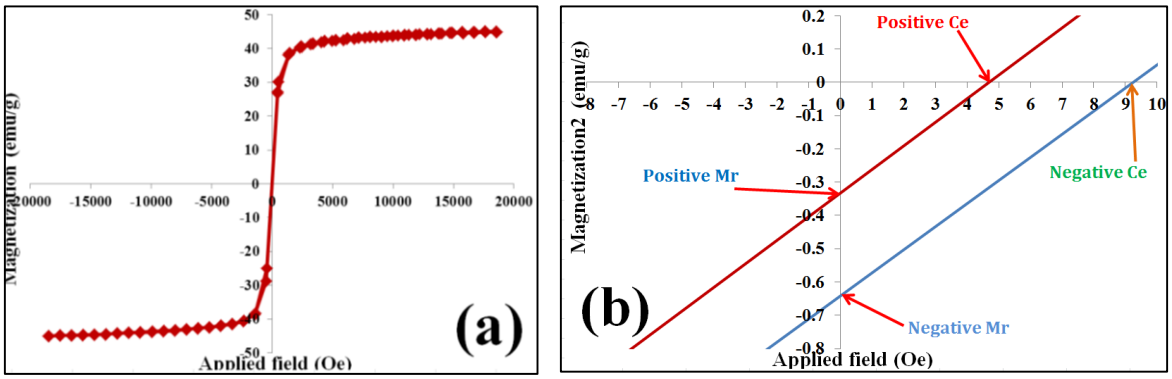

Fig. 4. (a) The measured M-H profile for the deposited IONs and (b) their hysteresis loop at the conditions of applied field →0

3.4. Magnetic evaluation

To determine the magnetic nature of the synthesized PVP-capped Cu^{2+}-doped Fe_3O_4 NPs, its magnetization values at the applied magnetic fields in the scale of -20000 Oe to +20000 Oe were recorded and the obtained values were plotted *vs.* applied field, as given in Fig. 5a. Furthermore, to provide the saturation magnetization (*Ms*), remanence (*Mr*) and coercivity (*Ce*) of prepared magnetic powder, the magnetization curve of powder was re-plotted at the small applied fields, i.e. magnetic field→0, as presented in Fig. 5b. Superparamagnetic nature of the fabricated magnetic powder is clearly verified from Fig. 5a, S-like form is seen for the VSM profile of the powder and also no hysteresis loop is existed in any zone of this curve. Table 1 lists the obtained *Ms*, *Mr* and *Ce* magnetic values. For better evaluation the magnetic ability of the prepared PVP/Cu-IONs powder, the magnetic data reported for the naked IONs are also inserted in Table 1from Refs. [22]. The synthesized PVP surface capped and crystal structure doped IONs showed *Ms*, *Ce* and *Mr* values of 45.01 emu/g, 7.1 Oe and 0.49 emu/g, respectively. The exhibited *Ms* value by the fabricated powder fall into the needed *Ms* range for biomedical uses like hyperthermia, drag delivery and MRI contrast agent [5-9]. Also, the negligible *Mr* and *Ce* value showed by our fabricated magnetic powder revealed its suitable superparamagnetic nature for the above mentioned biomedical aims. These magnetic are comparable with the reported ones for naked superparamagnetic iron oxide nanoparticles. Comparison to the naked IONs, the PVP/Cu-IONs have lower s*aturation magnetization* value

(as listed in Table 1), which is due to the non-magnetic PVP layer onto the surface of IONs and also the reduced magnetite weight in the fabricated IONs. However, the PVP/Cu-IONs presented lower remanence and coercivity values (i.e. *Mr*=0.33 emu/g and *Ce*=7.1 Oe) as compared with those reported for the naked IONs (i.e. *Mr*=0.95 emu/g and *Ce*=14.6 Oe). These findings verified better superparamagnetic nature of surface-capped, metal ion doped Fe_3O_4 NPs as compared to the undoped naked IONs. Hence, it was concluded that the superparamagnetic properties of magnetite nanoparticles are highly improved via PVP surface capping and structure doping with copper cations.

Table 1. Magnetic parameters measured through VSM analysis

Sample name	***Ms*** **(emu/g)**	**Coercivity (Oe)**	**Remanence (emu/g)**	**Negative *Mr* (emu/g)**	**Positive *Mr*(emu/g)**	**Positive *Ce* (Oe)**	**Negative *Ce* (Oe)**
Naked IONs [a]	72.96	14.6	0.95	0.83	2.73	-41.87	-12.66
PVP/Cu-IONs	45.01	7.1	0.49	-0.33	-0.65	4.88	9.14

[a] Inserted from Ref. [22]

4. CONCLUSION

In summary, a simple, one-step preparation procedure through the cathodic electrochemical deposition was constructed for the synthesis of iron oxide nanoparticles doped with copper cations and surface capped with PVP polymer. The TEM and XRD results verified the magnetite crystal phase and 5nm particle size for the fabricated iron oxide powder. Cu^{2+} doping (~7.5%wt.) into the deposited magnetite powder was supported by FT-IR and elemental results. Furthermore, PVP layer grafting onto the surface of the deposited magnetite nanoparticles was validated through FT-IR data. VSM studies indicated the superparamagnetic behavior of the fabricated PVP/Cu-IONs powder, where this powder showed the magnetic data of *Ms*=45.01 emu/g, *Ce*=7.1 Oe and *Mr*=0.49 emu/g. It was found that the fabricated magnetite particles have proper characteristic for biomedical aims.

REFERENCES

[1] L. S. Arias, J. P. Pessan, A. P. M. Vieira, T. M. Toito de Lima, A. C. Botazzo Delbem, and D. R. Monteiro, Antibiotics 7 (2018) 46.

[2] Y. L. Pang, S. Lim, H. C. Ong, and W. T. Chong, Ceram. Int. 42 (2016) 9.

[3] Y. Ha, S. Ko, I. Kim, Y. Huang, K. Mohanty, C. Huh, and J. A. Maynard, ACS Appl. Nano Mater. 1 (2018) 512.

[4] X. Li, J. Wei, K. E. Aifantis, Y. Fan, Q. Feng, F. Z. Cui, and F. Watari, J. Biomed. Mater. Res. 104A (2016) 1285.

[5] D. E. Lee, H. Koo, I. C. Sun, J. H. Ryu, K. Kim, and I. C. Kwon, Chem. Soc. Rev. 41 (2012) 2656.
[6] J. J. Giner-Casare, M. Henriksen-Lacey, M. Coronado-Puchau, and L. M. Liz-Marzan, Mater. Today 19 (2016) 19.
[7] R. M. Patil, P. B. Shete, N. D. Thorat, S. V. Otari, K. C. Barick, A. Prasad, R. S. Ningthoujam, B. M. Tiwale, and S. H. Pawar, J. Magn. Magn. Mater. 355 (2014) 22.
[8] M. Aghazadeh, I. Karimzadeh, and M. R. Ganjali, Curr. Nanosci. 15 (2019) 169.
[9] N. V. Srikanth Vallabani, and S. Singh, 3 Biotech 8 (2018) 279.
[10] X. Liu, S. Lu, D. Liu, L. Zhang, L. Zhang, X. Yu, and R. Liu, Brain Res. 1707 (2019) 141.
[11] V. Gómez-Vallejo, M. Puigivila, S. Plaza-García, B. Szczupak, R. Piñol, J. L. Murillo, V. Sorribas, G. Lou, S. Veintemillas, P. Ramos-Cabrerg, J. Llop, and A. Millán, Nanoscale 10 (2018) 14153.
[12] A. Espinosa, R. Di Corato, J. Kolosnjaj-Tabi, P. Flaud, T. Pellegrino, and C. Wilhelm, ACS Nano 10 (2016) 2436.
[13] J. Mosayebi, M. Kiyasatfar, and S. Laurent, Adv. Healthcare Mater. (2017) 1700306.
[14] M. Aghazadeh, A. Nozad, H. Adelkhani, and M. Ghaemi, J. Electrochem. Soc. 157 (2010) D519.
[15] M. Magro, D. Baratella, E. Bonaiuto, J. Almeida Roger, G. Chemello, S. Pasquaroli, L. Mancini, I. Olivotto, G. Zoppellaro, J. Ugolotti, C. Aparicio, A. P. Fifi, G. Cozza, G. Miotto, G. Radaelli, D. Bertotto, R. Zboril, and F. Vianello, Biomacromol. 20 (2019) 1375.
[16] M. Hosseini, M. Aghazadeh, and M. R. Ganjali, New J. Chem. 41 (2017) 12678.
[17] C. Tamez, R. Hernandez, and J. G. Parsons, Microchem. J. 125 (2016) 97.
[18] P. Saharan, G. R. Chaudhary, S. K. Mehta, and A. Umar, J. Nanosci. Nanotechnol. 14 (2014) 627.
[19] M. Aghazadeh, M. Hosseinifard, B. Sabour, and S. Dalvand, Appl. Surf. Sci. 287 (2013) 187.
[20] S. R. Pouran, A. A. Abdul Raman, W. Mohd Ashri, and W. Daud, J. Cleaner Production 64 (2014) 24.
[21] M. Munoz, Z. M. de Pedro, J. A. Casas, and J. J. Rodriguez, Appl. Catalysis B 176–177 (2015) 249.
[22] M. Aghazadeh, and M. R. Ganjali, Ceram. Int. 44 (2018) 520.
[23] M. Aghazadeh, and M. R. Ganjali, J. Mater. Sci. 53 (2018) 295.
[24] M. Aghazadeh, and M. R. Ganjali, J. Mater. Sci.: Mater. Electron. 29 (2018) 2291.
[25] M. Aghazadeh, I. Karimzadeh, M. R. Ganjali, and A. Behzad, J. Mater. Sci.: Mater. Electron. 28 (2017) 18121.
[26] M. Aghazadeh, I. Karimzadeh, and M. R. Ganjali, Mater. Lett. 209 (2017) 450.

[27] M. Aghazadeh, I. Karimzadeh, and M. R. Ganjali, J. Mater. Sci.: Mater. Electron. 28 (2017) 13532.
[28] N. Lee, D. Yoo, D. Ling, M. H. Cho, T. Hyeon, and J. Cheon, Chem. Rev. 115 (2015) 10637.
[29] Y. Hu, S. Mignani, J. P. Majoral, M. Shen, and X. Shi, Chem. Soc. Rev. 47 (2018) 1874.
[30] D. A. Brewster, D. J. Sarappa, and K. E. Knowles, Polyhedron 157 (2019) 54.
[31] W. Glasgow, B. Fellows, B. Qi, T. Darroudi, and O. T. Mefford, Particuology 26 (2016) 47.
[32] M. Aghazadeh, I Karimzadeh, M. R. Ganjali, J. Mater. Sci.: Mater. Electron. 29 (2018) 5163.
[33] X. D. Liu, H. Chen, S. S. Liu, L. Q. Ye, and Y. P. Li, Mater. Res. Bull. 62 (2015) 217.
[34] A. Radoń, A. Drygała, Ł. Hawełek, and D. Łukowiec, Mater. Characterization 131 (2017) 148.
[35] L. B. Mello, L. C. Varanda, F. A. Sigoli, and I. O. Mazali, J. Alloys Compd. 779 (2019) 698.
[36] R. Mout, D. F. Moyano, S. Rana, and V. M. Rotello, Chem. Soc. Rev. 41 (2012) 2539.
[37] K. Turcheniuk, A.V. Tarasevych, V.P. Kukhar, R. Boukherrouba, and S. Szunerits, Nanoscale 5 (2013) 10729.
[38] N. Erathodiyil, and J. Y. Ying, Acc. Chem. Res. 44 (2011) 925.
[39] M. Aghazadeh, I. Karimzadeh, M. R. Ganjali, D. Gharailou, and P. Kolivand, Curr. Nanosci. 13 (2017) 274.
[40] I. Karimzadeh, M. Aghazadeh, M. R. Ganjali, and T. Dourudi, Curr. Nanosci. 13 (2017) 167.
[41] Y. Zhang, J. Y. Liu, S. Ma, Y. J. Zhang, X. Zhao, X. D. Zhang, and Z. D. Zhang, J. Mater. Sci. Mater. Med. 21 (2010) 1205.
[42] M. Aghazadeh, I. Karimzadeh, and M. R. Ganjali, Mater. Lett. 228 (2018) 137.
[43] I. Karimzadeh, M. Aghazadeh, M. R. Ganjali, P. Norouzi, S. Shirvani-Arani, T. Doroudi, P. H. kolivand, S. A. Marashi, and D. Gharailou, Mater. Lett. 179 (2016) 5.
[44] M. Aghazadeh, and M. R. Ganjali, J. Mater. Sci.: Mater. Electron. 28 (2017) 8144.
[45] R. Y. Hong, B. Feng, L. L. Chen, G. H. Liu, H. Z. Li, Y. Zheng, and D. G. Wei, Biochem. Engin. J. 42 3 (2008) 290.
[46] T. Yousefi, A.N. Golikand, M.H. Mashhadizadeh, and M. Aghazadeh, Curr. Appl. Phys. 12 (2012) 544.
[47] M. Aghazadeh, and I. Karimzadeh, Curr. Nanosci. 14 (2018) 42.
[48] E. Shah, P. Upadhyay, M. Singh, M. Shoab Mansuri, R. Begum, N. Shethd, and H. P. Soni, New J. Chem. 40 (2016) 9507.
[49] A. G. Magdalena, I. M. B. Silva, R. F. C. Marques, A. R. F. Pipi, and M. Jafelicci, J. Phys. Chem. Solids 113 (2018) 5.

[50] M. Aghazadeh, I. Karimzadeh, M. R. Ganjali, and M. M. Morad, Mater. Lett. 196 (2017) 392.
[51] I. Karimzadeh, M. Aghazadeh, M. R. Ganjali, P. Norouzi, T. Doroudi, and P. H. Kolivand, Mater. Lett. 189 (2017) 290.
[52] M. Aghazadeh, and M. R. Ganjali, J. Mater. Sci.: Mater. Electron. 28 (2017) 11406.
[53] M. Aghazadeh, A. Rashidi, and M. R. Ganjali, Electron. Mater. Lett. 14 (2018) 37.
[54] M. Aghazadeh, M. Ghaemi, A. N. Golikand, and A. Ahmadi, Mater. Lett. 65 (2011) 2545.
[55] M. Aghazadeh, M. R. Ganjali, and P. Norouzi, Mater. Res. Express 3 (2016) 055013.
[56] M. Aghazadeh, T. Yousefi, and M Ghaemi, J. Rare Earths 30 (2012) 236.
[57] J. Talat Mehrabad, M. Aghazadeh, M. Ghannadi Maragheh, M. R. Ganjali, and P. Norouzi, Mater. Lett. 184 (2016) 223.
[58] M. Aghazadeh, and I. Karimzadeh, Mater. Res. Express 4 (2017) 105505.
[59] J. Tizfahm, M. Aghazadeh, M. G. Maragheh, M. R. Ganjali, P. Norouzi, and F. Faridbod, Mater. Lett. 167 (2016) 153.
[60] M. Aghazadeh, J. Mater. Sci.: Mater. Electron. 28 (2017) 3108.
[61] M. Aghazadeh, A. Rashidi, and M. R. Ganjali, Int. J. Electrochem. Sci. 11 (2016) 11002.
[62] M. Aghazadeh, I. Karimzadeh, A. Ahmadi, and M. R. Ganjali, J. Mater. Sci.: Mater. Electron. 29 (2018) 14567.
[63] M. Aghazadeh, I. Karimzadeh, A. Ahmadi, M. R. Ganjali, and P. Norouzi, J. Mater. Sci.: Mater. Electron. 29 (2018) 14378.
[64] M Aghazadeh, Anal. Bioanal. Electrochem. 10 (2018) 554.
[65] M. Aghazadeh, Anal. Bioanal. Electrochem. 11 (2019) 211.
[66] M. Aghazadeh, and M.R. Ganjali, J. Mater. Sci.: Mater. Electron. 29 (2018) 4981.
[67] M. Aghazadeh, J. Mater. Sci.: Mater. Electron. 28 (2017) 18755.
[68] M. Aghazadeh, I. Karimzadeh, and M. R. Ganjali, J. Mater. Sci.: Mater. Electron. 28 (2017) 19061.
[69] M. Aghazadeh, and S. Dalvand, J. Electrochem. Soc. 161 (2014) D18.
[70] M. Aghazadeh, I. Karimzadeh, and M. R. Ganjali, J. Electron. Mater. 47 (2018) 3026.
[71] M. Aghazadeh, M. G. Maragheh, M. R. Ganjali, and P. Norouzi, Inorg. Nano-Metal Chem. 27 (2017) 1085.
[72] M. Aghazadeh, Mater. Lett. 211 (2018) 225.
[73] M. Aghazadeh, A. N. Golikand, M. Ghaemi, and T. Yousefi, Mater. Lett. 65 (2011) 1466.